

The low-temperature spin-glass phase

Sample-dependent parallel tempering on the Janus computer

David Yllanes for the **Janus Collaboration**¹

Dep. Física Teórica, Universidad Complutense de Madrid

<http://teorica.fis.ucm.es/grupos/grupo-TEC.html>

J. Stat. Mech. (2010) P06026 and arXiv:1003.2943

Melbourne, 26 July 2010

¹ R. Alvarez Baños, A. Cruz, L.A. Fernandez, J.M. Gil-Narvion, A. Gordillo-Guerrero, M. Guidetti, A. Maiorano, F. Mantovani, E. Marinari, V. Martin-Mayor, J. Monforte-Garcia, A. Muñoz Sudupe, D. Navarro, G. Parisi, S. Perez-Gaviro, J.J. Ruiz-Lorenzo, S.F. Schifano, B. Seoane, A. Tarancon, R. Tripicciono and D. Yllanes

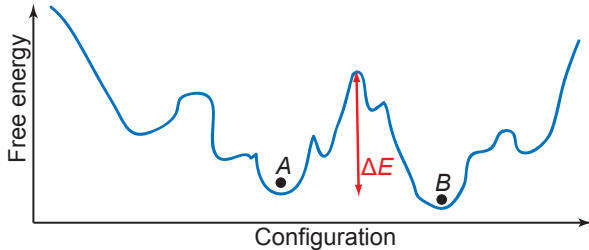
- 1 Achieving thermalisation
- 2 Assessing thermalisation
- 3 Physics results

1 Achieving thermalisation

2 Assessing thermalisation

3 Physics results

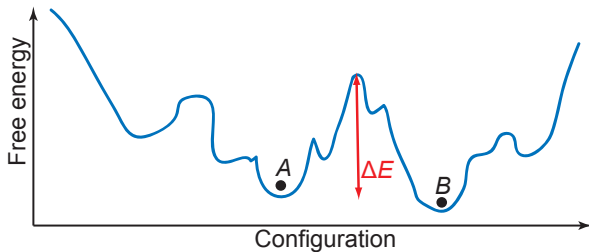
Introduction



Simulating disordered systems

- Rugged free-energy landscapes

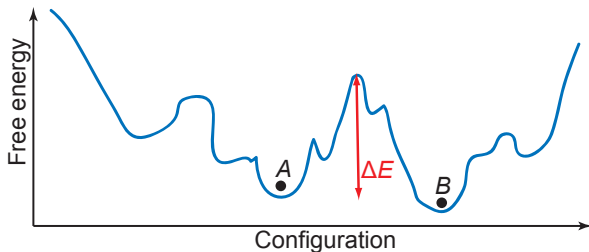
Introduction



Simulating disordered systems

- Rugged free-energy landscapes
 - Many valleys, separated by large energy barriers.
 - The dynamics at low T is exceedingly slow.

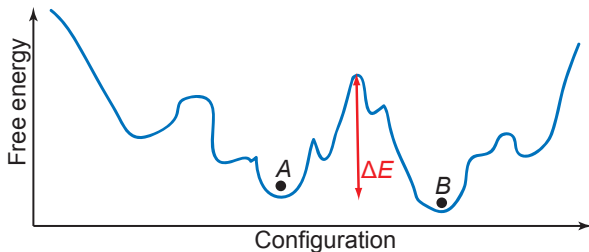
Introduction



Simulating disordered systems

- Rugged free-energy landscapes
⇒ long simulations to thermalise.

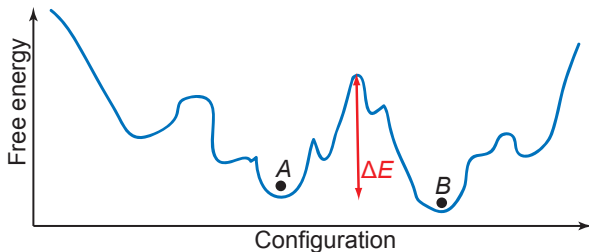
Introduction



Simulating disordered systems

- Rugged free-energy landscapes
⇒ long simulations to thermalise.
- Statistical errors dominated by sample-to-sample fluctuations

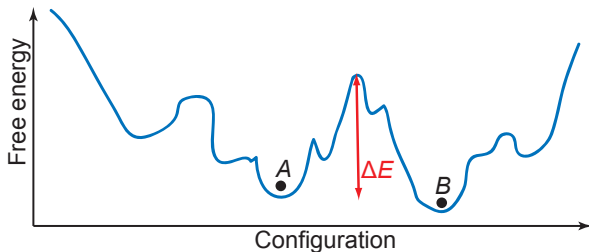
Introduction



Simulating disordered systems

- Rugged free-energy landscapes
⇒ long simulations to thermalise.
- Statistical errors dominated by sample-to-sample fluctuations
⇒ avoid overlong simulations and thermalise many samples

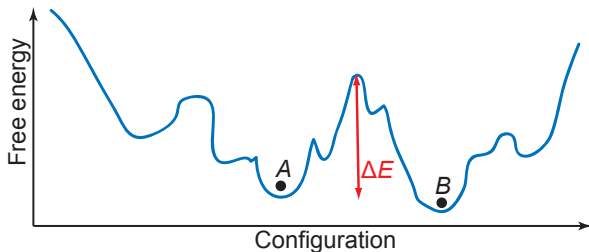
Introduction



Simulating disordered systems

- Rugged free-energy landscapes
⇒ long simulations to thermalise.
- Statistical errors dominated by sample-to-sample fluctuations
⇒ avoid overlong simulations and thermalise many samples
- We need

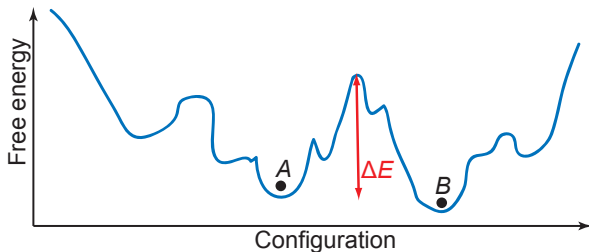
Introduction



Simulating disordered systems

- Rugged free-energy landscapes
⇒ long simulations to thermalise.
- Statistical errors dominated by sample-to-sample fluctuations
⇒ avoid overlong simulations and thermalise many samples
- We need
 - Fast computers & efficient algorithms to achieve thermalisation.

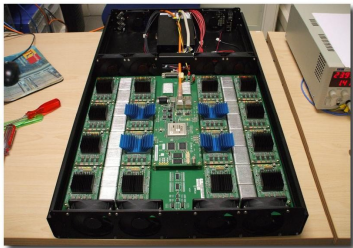
Introduction



Simulating disordered systems

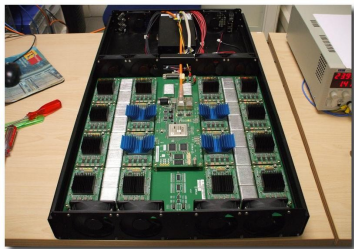
- Rugged free-energy landscapes
⇒ long simulations to thermalise.
- Statistical errors dominated by sample-to-sample fluctuations
⇒ avoid overlong simulations and thermalise many samples
- We need
 - Fast computers & efficient algorithms to achieve thermalisation.
 - A reliable method to choose the simulation length.

The Janus computer

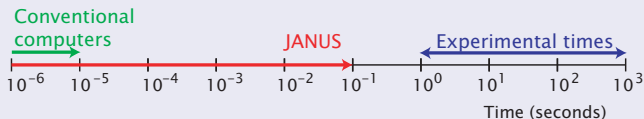


- **Janus** is a custom built computing system, made of FPGAs:
 - Massively parallel
 - Reconfigurable
 - Made of modules

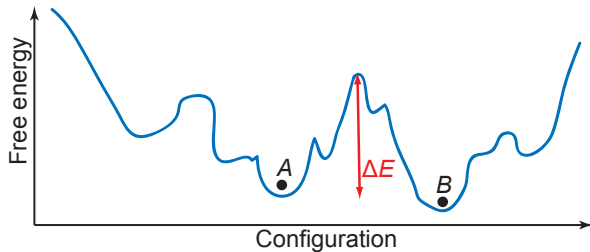
The Janus computer



- **Janus** is a custom built computing system, made of FPGAs:
 - Massively parallel
 - Reconfigurable
 - Made of modules
- We outperform conventional PCs by several orders of magnitude.

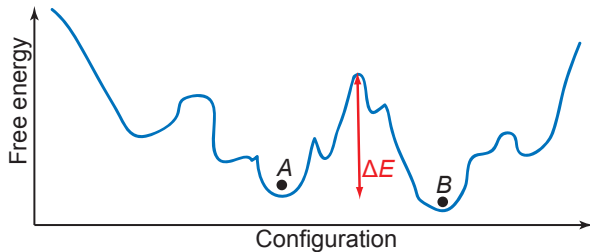


The parallel tempering algorithm



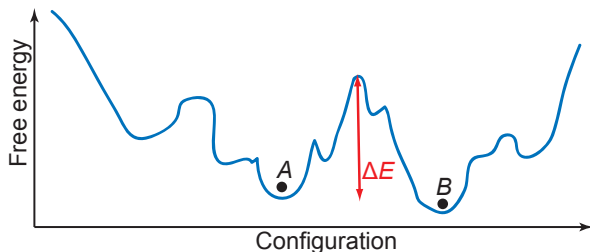
- The same energy barriers that are difficult to cross at T_1 are easy to overcome at $T_2 > T_1$.

The parallel tempering algorithm



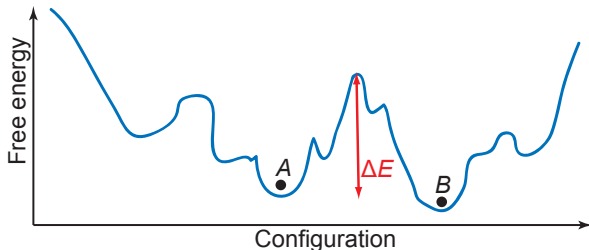
- The same energy barriers that are difficult to cross at T_1 are easy to overcome at $T_2 > T_1$.

The parallel tempering algorithm



- The same energy barriers that are difficult to cross at T_1 are easy to overcome at $T_2 > T_1$.
- Simulate N_T copies of the system at several temperatures.

The parallel tempering algorithm



- The same energy barriers that are difficult to cross at T_1 are easy to overcome at $T_2 > T_1$.
- Simulate N_T copies of the system at several temperatures.
- Every N_{PT} heat-bath steps, try to exchange configurations at neighbouring temperatures with probability

$$p = \min\{1, \exp[-(\beta_{i+1} - \beta_i)(E_{i+1} - E_i)]\}$$

- The temperature of each copy performs a random walk in T space.

Our simulations

L	T_{\min}	T_{\max}	N_T	N_{MC}^{\min}	N_{MC}^{\max}
8	0.150	1.575	10	5×10^6	8.30×10^8
12	0.414	1.575	12	1×10^7	1.53×10^{10}
16	0.479	1.575	16	4×10^8	2.79×10^{11}
24	0.625	1.600	28	1×10^9	1.81×10^{12}
32	0.703	1.574	34	4×10^9	7.68×10^{11}

The model and our parameters

- $\mathcal{H} = - \sum_{\langle x,y \rangle} J_{xy} \sigma_x \sigma_y$, $P(J_{xy}) = \delta(J_{xy}^2 - 1)$.
- We thermalise $L = 32$ down to $T = 0.703 \simeq 0.64 T_c$.
- 4000 samples for $L \leq 24$ and 1000 samples for $L = 32$.
- Parallel tempering with sample-dependent simulation times.
- A total of 1.1×10^{20} spin updates.

1 Achieving thermalisation

2 Assessing thermalisation

3 Physics results

Autocorrelation times

- Robust thermalisation check \rightarrow compute autocorrelation times τ :

$$C_O(t) = \langle [O(0) - \langle O \rangle][O(t) - \langle O \rangle] \rangle, \quad \rho_O(t) = C_O(t)/C_O(0)$$

Autocorrelation times

- Robust thermalisation check \rightarrow compute autocorrelation times τ :

$$C_O(t) = \langle [O(0) - \langle O \rangle][O(t) - \langle O \rangle] \rangle, \quad \rho_O(t) = C_O(t)/C_O(0)$$

$$\tau_{\text{int}} = \frac{1}{2} + \sum_t \rho_O(t)$$

Autocorrelation times

- Robust thermalisation check \rightarrow compute autocorrelation times τ :

$$C_O(t) = \langle [O(0) - \langle O \rangle][O(t) - \langle O \rangle] \rangle, \quad \rho_O(t) = C_O(t)/C_O(0)$$

$$\tau_{\text{int}} = \frac{1}{2} + \sum_t \rho_O(t)$$

$$\rho_O(t) = A e^{-t/\tau_{\text{exp}}} + \sum_i A_i e^{-t/\tau_i}, \quad (\tau_{\text{exp}} > \tau_i : \text{relaxation time})$$

Autocorrelation times

- Robust thermalisation check \rightarrow compute autocorrelation times τ :

$$C_O(t) = \langle [O(0) - \langle O \rangle][O(t) - \langle O \rangle] \rangle, \quad \rho_O(t) = C_O(t)/C_O(0)$$

$$\tau_{\text{int}} = \frac{1}{2} + \sum_t \rho_O(t)$$

$$\rho_O(t) = A e^{-t/\tau_{\text{exp}}} + \sum_i A_i e^{-t/\tau_i}, \quad (\tau_{\text{exp}} > \tau_i : \text{relaxation time})$$

Autocorrelation times

- Robust thermalisation check \rightarrow compute autocorrelation times τ :

$$C_O(t) = \langle [O(0) - \langle O \rangle][O(t) - \langle O \rangle] \rangle, \quad \rho_O(t) = C_O(t)/C_O(0)$$

$$\tau_{\text{int}} = \frac{1}{2} + \sum_t \rho_O(t)$$

$$\rho_O(t) = A e^{-t/\tau_{\text{exp}}} + \sum_i A_i e^{-t/\tau_i}, \quad (\tau_{\text{exp}} > \tau_i : \text{relaxation time})$$

- This requires very long simulations (orders of magnitude greater than τ).

Autocorrelation times

- Robust thermalisation check \rightarrow compute autocorrelation times τ :

$$C_O(t) = \langle [O(0) - \langle O \rangle][O(t) - \langle O \rangle] \rangle, \quad \rho_O(t) = C_O(t)/C_O(0)$$

$$\tau_{\text{int}} = \frac{1}{2} + \sum_t \rho_O(t)$$

$$\rho_O(t) = A e^{-t/\tau_{\text{exp}}} + \sum_i A_i e^{-t/\tau_i}, \quad (\tau_{\text{exp}} > \tau_i : \text{relaxation time})$$

- This requires very long simulations (orders of magnitude greater than τ).
- OK for ordered systems.

Autocorrelation times

- Robust thermalisation check \rightarrow compute autocorrelation times τ :

$$C_O(t) = \langle [O(0) - \langle O \rangle][O(t) - \langle O \rangle] \rangle, \quad \rho_O(t) = C_O(t)/C_O(0)$$

$$\tau_{\text{int}} = \frac{1}{2} + \sum_t \rho_O(t)$$

$$\rho_O(t) = A e^{-t/\tau_{\text{exp}}} + \sum_i A_i e^{-t/\tau_i}, \quad (\tau_{\text{exp}} > \tau_i : \text{relaxation time})$$

- This requires very long simulations (orders of magnitude greater than τ).
- OK for ordered systems.
- Not practical for disordered systems (the main source of error is sample-to-sample fluctuation).

Assessing thermalisation in disordered systems

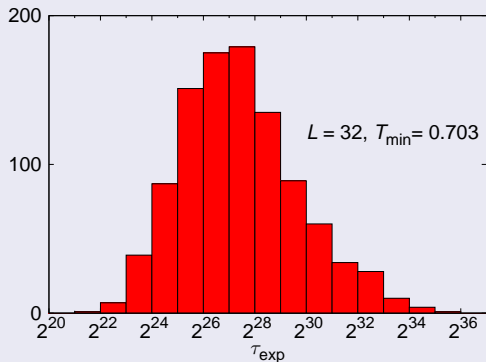
Traditional method

- Study the time evolution of **disorder averages** in a logarithmic scale.
- If the last few bins show no evolution, the system is thermalised.

Assessing thermalisation in disordered systems

Traditional method

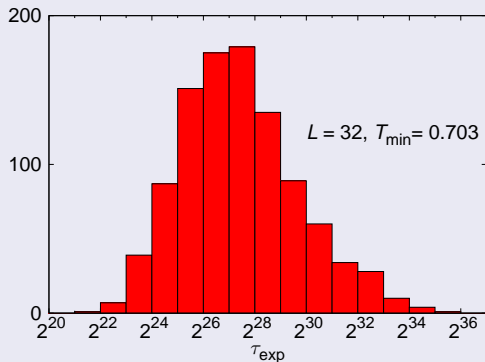
- Study the time evolution of **disorder averages** in a logarithmic scale.
- If the last few bins show no evolution, the system is thermalised.
- Problem: the thermalisation time is wildly sample dependent:



Assessing thermalisation in disordered systems

Traditional method

- Study the time evolution of **disorder averages** in a logarithmic scale.
- If the last few bins show no evolution, the system is thermalised.
- Problem: the thermalisation time is wildly sample dependent:



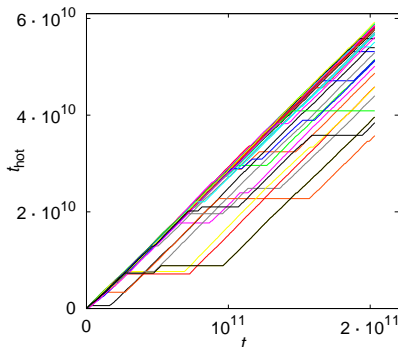
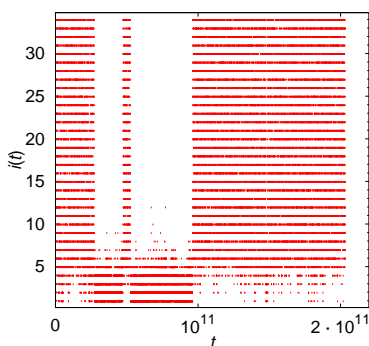
It is not efficient (or safe!)
to use the same
simulation time for all samples.

The temperature random walk

- The use of parallel tempering provides an alternative way of ensuring thermalisation \longrightarrow use the dynamics of the temperature random walk.

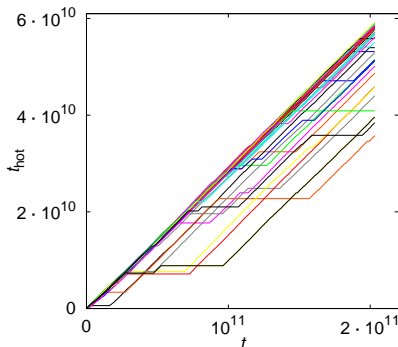
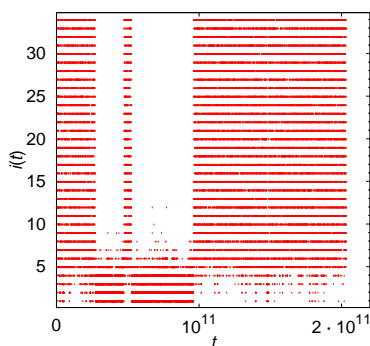
The temperature random walk

- The use of parallel tempering provides an alternative way of ensuring thermalisation \rightarrow use the dynamics of the temperature random walk.



The temperature random walk

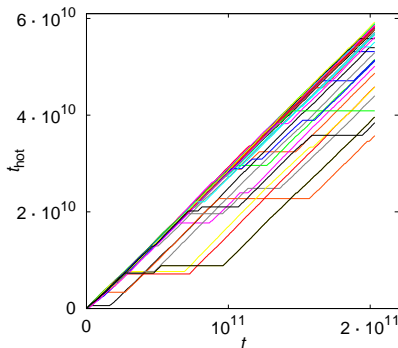
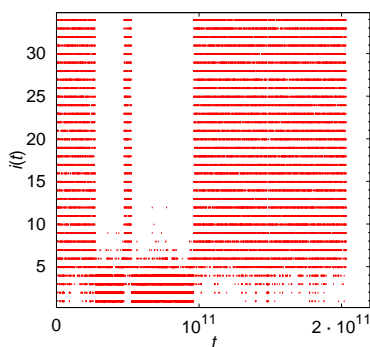
- The use of parallel tempering provides an alternative way of ensuring thermalisation \rightarrow use the dynamics of the temperature random walk.



- All the configurations must cover the whole temperature range.

The temperature random walk

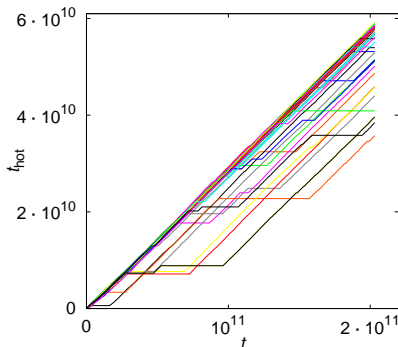
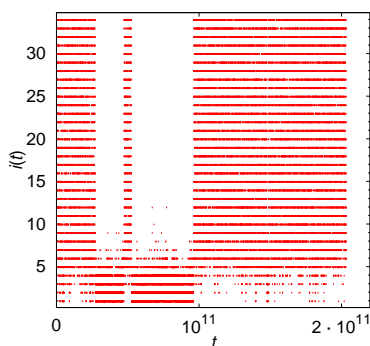
- The use of parallel tempering provides an alternative way of ensuring thermalisation \rightarrow use the dynamics of the temperature random walk.



- All the configurations must cover the whole temperature range.
- Samples with long thermalisation times will have long plateaux.

The temperature random walk

- The use of parallel tempering provides an alternative way of ensuring thermalisation \rightarrow use the dynamics of the temperature random walk.



- All the configurations must cover the whole temperature range.
- Samples with long thermalisation times will have long plateaux.
- We can quantify this idea to provide a robust thermalisation test.

Quantifying the temperature random walk (I)

- For each configuration we have a temperature index, indicating its temperature at time t

$$i(t) \in \{1, 2, \dots, N_T\}, \quad T_1 < T_2 < \dots < T_c < \dots < T_{N_T}$$

Quantifying the temperature random walk (I)

- For each configuration we have a temperature index, indicating its temperature at time t

$$i(t) \in \{1, 2, \dots, N_T\}, \quad T_1 < T_2 < \dots < T_c < \dots < T_{N_T}$$

- We define a mapping f such that

$f(i)$ changes signs at i_{T_c} , and only there

Quantifying the temperature random walk (I)

- For each configuration we have a temperature index, indicating its temperature at time t

$$i(t) \in \{1, 2, \dots, N_T\}, \quad T_1 < T_2 < \dots < T_c < \dots < T_{N_T}$$

- We define a mapping f such that

$f(i)$ changes signs at i_{T_c} , and only there

$$\sum_{i=1}^{N_T} f(i) = 0$$

Quantifying the temperature random walk (I)

- For each configuration we have a temperature index, indicating its temperature at time t

$$i(t) \in \{1, 2, \dots, N_T\}, \quad T_1 < T_2 < \dots < T_c < \dots < T_{N_T}$$

- We define a mapping f such that

$$f(i) \text{ changes signs at } i_{T_c}, \text{ and only there} \quad \sum_{i=1}^{N_T} f(i) = 0$$

Temperatures symmetric with respect to $T_c \longrightarrow$ choose linear f

Quantifying the temperature random walk (I)

- For each configuration we have a temperature index, indicating its temperature at time t

$$i(t) \in \{1, 2, \dots, N_T\}, \quad T_1 < T_2 < \dots < T_c < \dots < T_{N_T}$$

- We define a mapping f such that

$$f(i) \text{ changes signs at } i_{T_c}, \text{ and only there} \quad \sum_{i=1}^{N_T} f(i) = 0$$

Temperatures symmetric with respect to T_c \longrightarrow choose linear f

- We can now compute the autocorrelation of f , averaging over all configurations and replicas \longrightarrow we do not need so long a run.

Quantifying the temperature random walk (I)

- For each configuration we have a temperature index, indicating its temperature at time t

$$i(t) \in \{1, 2, \dots, N_T\}, \quad T_1 < T_2 < \dots < T_c < \dots < T_{N_T}$$

- We define a mapping f such that

$$f(i) \text{ changes signs at } i_{T_c}, \text{ and only there} \quad \sum_{i=1}^{N_T} f(i) = 0$$

Temperatures symmetric with respect to $T_c \rightarrow$ choose linear f

- We can now compute the autocorrelation of f , averaging over all configurations and replicas \rightarrow we do not need so long a run.
- The integrated autocorrelation time is now easy to compute.

Quantifying the temperature random walk (I)

- For each configuration we have a temperature index, indicating its temperature at time t

$$i(t) \in \{1, 2, \dots, N_T\}, \quad T_1 < T_2 < \dots < T_c < \dots < T_{N_T}$$

- We define a mapping f such that

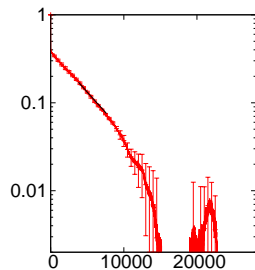
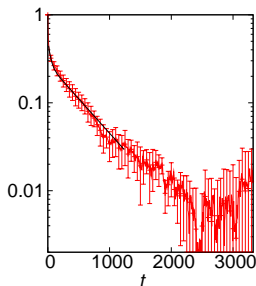
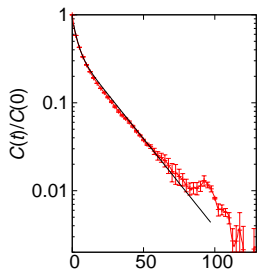
$$f(i) \text{ changes signs at } i_{T_c}, \text{ and only there} \quad \sum_{i=1}^{N_T} f(i) = 0$$

Temperatures symmetric with respect to T_c \longrightarrow choose linear f

- We can now compute the autocorrelation of f , averaging over all configurations and replicas \longrightarrow we do not need so long a run.
- The integrated autocorrelation time is now easy to compute.
- For critical-point studies $\tau_{\text{int}} \simeq \tau_{\text{exp}}$ \longrightarrow use τ_{int} to assess thermalisation. First used in L.A. Fernandez et al., PRE **80**, 051105 (2009) (A.P. Young's talk).

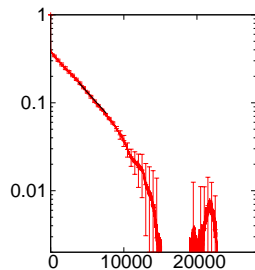
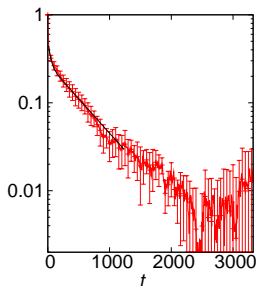
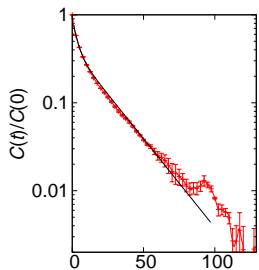
Quantifying the temperature random walk (II)

- At low temperatures, the correlation functions are more complicated:



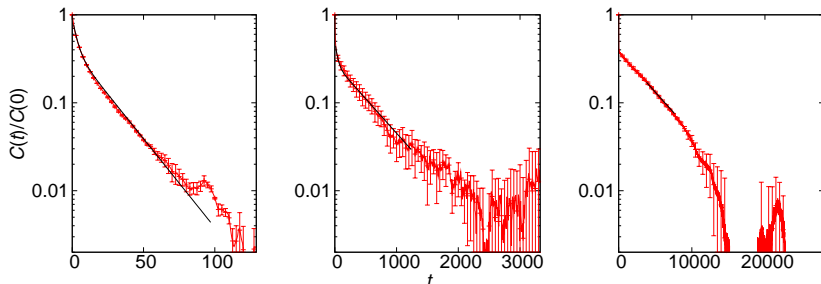
Quantifying the temperature random walk (II)

- At low temperatures, the correlation functions are more complicated:



Quantifying the temperature random walk (II)

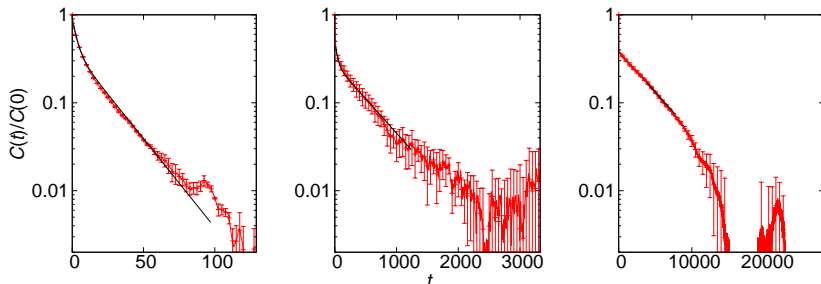
- At low temperatures, the correlation functions are more complicated:



- We parameterise $C(t) \simeq Ae^{-t/\tau_{\text{exp}}} + A_1e^{-t/\tau_1}$ and perform a double fit.

Quantifying the temperature random walk (II)

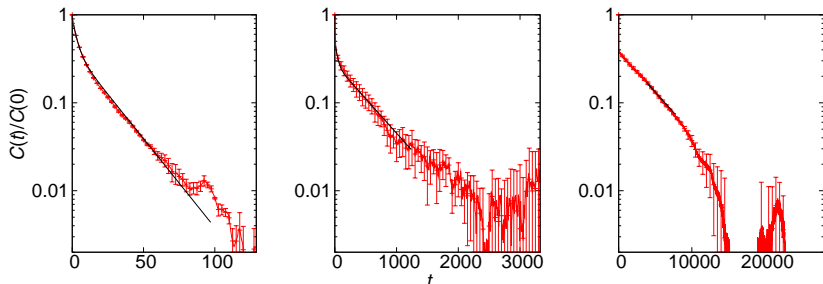
- At low temperatures, the correlation functions are more complicated:



- We parameterise $C(t) \simeq Ae^{-t/\tau_{\text{exp}}} + A_1e^{-t/\tau_1}$ and perform a double fit.
- The fitting range is chosen automatically, based on τ_{int} .

Quantifying the temperature random walk (II)

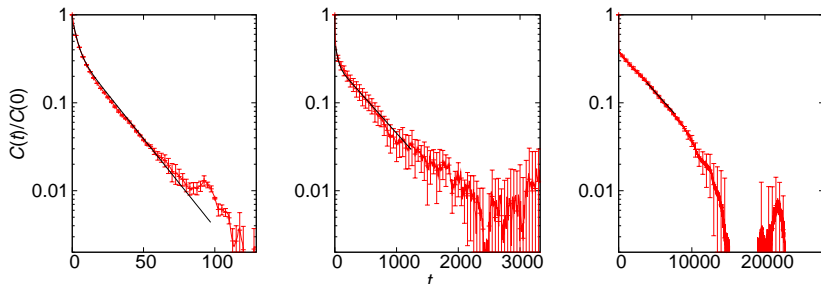
- At low temperatures, the correlation functions are more complicated:



- We parameterise $C(t) \simeq Ae^{-t/\tau_{\text{exp}}} + A_1e^{-t/\tau_1}$ and perform a double fit.
- The fitting range is chosen automatically, based on τ_{int} .
- Thermalisation protocol:
 - 1 Simulate all samples for N_{min} steps (enough to measure $C(t)$).

Quantifying the temperature random walk (II)

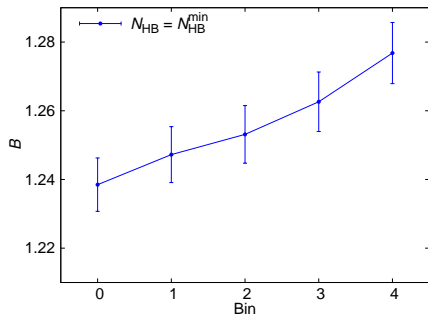
- At low temperatures, the correlation functions are more complicated:



- We parameterise $C(t) \simeq Ae^{-t/\tau_{\text{exp}}} + A_1e^{-t/\tau_1}$ and perform a double fit.
- The fitting range is chosen automatically, based on τ_{int} .
- Thermalisation protocol:
 - 1 Simulate all samples for N_{min} steps (enough to measure $C(t)$).
 - 2 Compute τ_{exp} and extend the each run so that $N > 12\tau_{\text{exp}}$.

Thermalisation tests

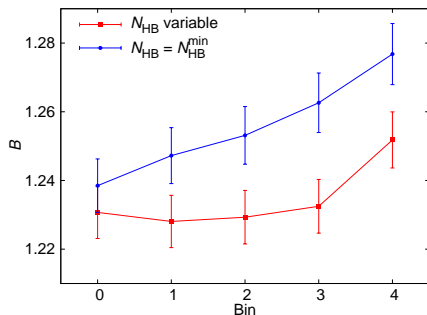
- Our simulations satisfy the traditional thermalisation tests:



(Logarithmic bins: 0 = second half, 1 = second quarter, etc.)

Thermalisation tests

- Our simulations satisfy the traditional thermalisation tests:

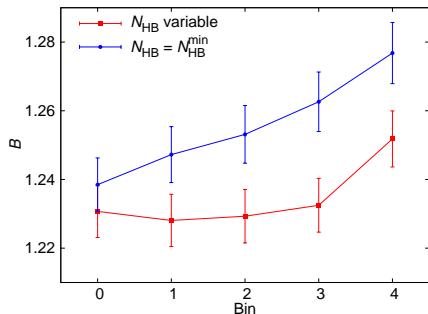


(Logarithmic bins: 0 = second half, 1 = second quarter, etc.)

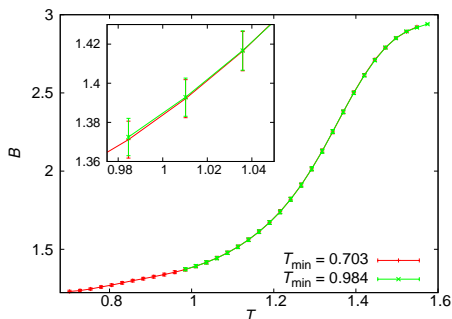
- The increase in CPU time from the blue to the red curve is only 150%, yet by correctly allocating it we obtain several stable logarithmic bins.

Thermalisation tests

- Our simulations satisfy the traditional thermalisation tests:



(Logarithmic bins: 0 = second half, 1 = second quarter, etc.)



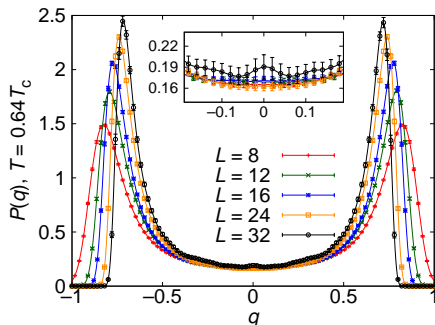
- The increase in CPU time from the blue to the red curve is only 150%, yet by correctly allocating it we obtain several stable logarithmic bins.

1 Achieving thermalisation

2 Assessing thermalisation

3 **Physics results**

The probability distribution of the order parameter

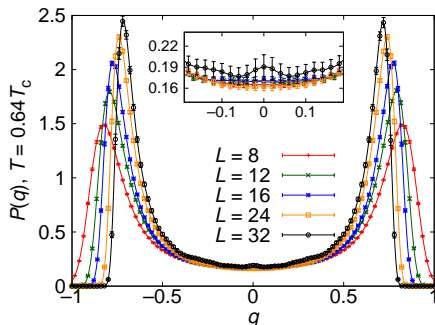


- Our order parameter is the overlap q

$$q = \frac{1}{V} \sum_x q_x = \frac{1}{V} \sum_x \sigma_x^{(1)} \sigma_x^{(2)}$$

- Its pdf $P(q)$ has peaks at $\pm q_{EA}$.

The probability distribution of the order parameter



- Our order parameter is the overlap q

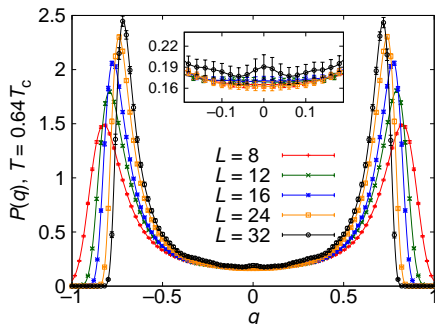
$$q = \frac{1}{V} \sum_x q_x = \frac{1}{V} \sum_x \sigma_x^{(1)} \sigma_x^{(2)}$$

- Its pdf $P(q)$ has peaks at $\pm q_{EA}$.
- There are several conflicting theoretical pictures for $P(q)$ in the thermodynamical limit:

Droplet $P(q) = \delta(q_{EA}^2 - q^2)$.

RSB Non-zero probability density in $|q| < q_{EA}$.

The probability distribution of the order parameter



- Our order parameter is the overlap q

$$q = \frac{1}{V} \sum_x q_x = \frac{1}{V} \sum_x \sigma_x^{(1)} \sigma_x^{(2)}$$

- Its pdf $P(q)$ has peaks at $\pm q_{EA}$.
- There are several conflicting theoretical pictures for $P(q)$ in the thermodynamical limit:

Droplet $P(q) = \delta(q_{EA}^2 - q^2)$.

RSB Non-zero probability density in $|q| < q_{EA}$.

- q_{EA} very difficult to compute.

Clustering states and fixed- q correlation functions

- In the RSB picture, the spin-glass phase is composed of a multiplicity of **clustering states**.

Clustering states and fixed- q correlation functions

- In the RSB picture, the spin-glass phase is composed of a multiplicity of **clustering states**.
- We isolate clustering states by considering correlations at fixed $q = c$

$$\tilde{C}_4(r|c) = \frac{\langle \sum_x q_x q_{x+r} \delta(q - c) \rangle}{\langle \delta(q - c) \rangle}$$

Clustering states and fixed- q correlation functions

- In the RSB picture, the spin-glass phase is composed of a multiplicity of **clustering states**.
- We isolate clustering states by considering correlations at fixed $q = c$

$$\frac{\langle \sum_x q_x q_{x+r} \delta(q - c) \rangle}{\langle \delta(q - c) \rangle} \xrightarrow[\text{convolution}]{\text{Gaussian}} C_4(r|c) = \frac{\langle \sum_x q_x q_{x+r} \exp[-V(q - c)^2/2] \rangle}{V \langle \exp[-V(q - c)^2/2] \rangle}$$

- We smooth the comb-like $P(q)$ with a Gaussian convolution.

Clustering states and fixed- q correlation functions

- In the RSB picture, the spin-glass phase is composed of a multiplicity of **clustering states**.
- We isolate clustering states by considering correlations at fixed $q = c$

$$\frac{\langle \sum_x q_x q_{x+r} \delta(q - c) \rangle}{\langle \delta(q - c) \rangle} \xrightarrow[\text{convolution}]{\text{Gaussian}} C_4(r|c) = \frac{\langle \sum_x q_x q_{x+r} \exp[-V(q - c)^2/2] \rangle}{V \langle \exp[-V(q - c)^2/2] \rangle}$$

- We smooth the comb-like $P(q)$ with a Gaussian convolution.
- For $T < T_c$ and $|q| \leq q_{EA}$ one expects

$$C_4(r|q) \simeq q^2 + \frac{A_q}{r^{\theta(q)}}$$

Clustering states and fixed- q correlation functions

- In the RSB picture, the spin-glass phase is composed of a multiplicity of **clustering states**.
- We isolate clustering states by considering correlations at fixed $q = c$

$$\frac{\langle \sum_x q_x q_{x+r} \delta(q - c) \rangle}{\langle \delta(q - c) \rangle} \xrightarrow[\text{convolution}]{\text{Gaussian}} C_4(r|c) = \frac{\langle \sum_x q_x q_{x+r} \exp[-V(q - c)^2/2] \rangle}{V \langle \exp[-V(q - c)^2/2] \rangle}$$

- We smooth the comb-like $P(q)$ with a Gaussian convolution.
- For $T < T_c$ and $|q| \leq q_{EA}$ one expects

$$C_4(r|q) \simeq q^2 + \frac{A_q}{r^{\theta(q)}}$$

- In real space, one has to perform a subtraction that complicates the analysis.

Correlations in Fourier space

- We consider instead the Fourier transform of $C_4(\mathbf{r}|q)$

$$\hat{C}_4(\mathbf{k}|q^2 < q_{\text{EA}}^2) \propto k^{\theta(q)-D} + \dots \quad \hat{C}_4(\mathbf{k}|q^2 > q_{\text{EA}}^2) \propto \frac{1}{k^2 + \xi_q^{-2}}$$

Correlations in Fourier space

- We consider instead the Fourier transform of $C_4(\mathbf{r}|q)$

$$\hat{C}_4(\mathbf{k}|q^2 < q_{\text{EA}}^2) \propto k^{\theta(q)-D} + \dots \quad \hat{C}_4(\mathbf{k}|q^2 > q_{\text{EA}}^2) \propto \frac{1}{k^2 + \xi_q^{-2}}$$

- We use the shorthand

$$F_q = \hat{C}_4(\mathbf{k}_{\text{min}}|q) \quad F_q^{(n)} = \hat{C}_4(n\mathbf{k}_{\text{min}}|q)$$

Correlations in Fourier space

- We consider instead the Fourier transform of $C_4(\mathbf{r}|q)$

$$\hat{C}_4(\mathbf{k}|q^2 < q_{\text{EA}}^2) \propto k^{\theta(q)-D} + \dots \quad \hat{C}_4(\mathbf{k}|q^2 > q_{\text{EA}}^2) \propto \frac{1}{k^2 + \xi_q^{-2}}$$

- We use the shorthand

$$F_q = \hat{C}_4(\mathbf{k}_{\text{min}}|q) \quad F_q^{(n)} = \hat{C}_4(n\mathbf{k}_{\text{min}}|q)$$

- Droplet and RSB disagree in the precise form of $\theta(q)$

Correlations in Fourier space

- We consider instead the Fourier transform of $C_4(\mathbf{r}|q)$

$$\hat{C}_4(\mathbf{k}|q^2 < q_{EA}^2) \propto k^{\theta(q)-D} + \dots \quad \hat{C}_4(\mathbf{k}|q^2 > q_{EA}^2) \propto \frac{1}{k^2 + \xi_q^{-2}}$$

- We use the shorthand

$$F_q = \hat{C}_4(\mathbf{k}_{\min}|q) \quad F_q^{(n)} = \hat{C}_4(n\mathbf{k}_{\min}|q)$$

- Droplet and RSB disagree in the precise form of $\theta(q)$
- Yet, both theories agree that a crossover appears in F_q for finite L

$$F_q \sim L^{D-\theta(q)} \quad \text{for } |q| < q_{EA} \quad \longrightarrow \quad F_q \sim 1 \quad \text{for } |q| > q_{EA}$$

Correlations in Fourier space

- We consider instead the Fourier transform of $C_4(\mathbf{r}|q)$

$$\hat{C}_4(\mathbf{k}|q^2 < q_{EA}^2) \propto k^{\theta(q)-D} + \dots \quad \hat{C}_4(\mathbf{k}|q^2 > q_{EA}^2) \propto \frac{1}{k^2 + \xi_q^{-2}}$$

- We use the shorthand

$$F_q = \hat{C}_4(\mathbf{k}_{\min}|q) \quad F_q^{(n)} = \hat{C}_4(n\mathbf{k}_{\min}|q)$$

- Droplet and RSB disagree in the precise form of $\theta(q)$
- Yet, both theories agree that a crossover appears in F_q for finite L

$$F_q \sim L^{D-\theta(q)} \quad \text{for } |q| < q_{EA} \quad \longrightarrow \quad F_q \sim 1 \quad \text{for } |q| > q_{EA}$$

- For large L the crossover becomes a phase transition where

$$\xi_q^{L=\infty} \propto (q^2 - q_{EA}^2)^{-\hat{\nu}}$$

(analogous to the study of the equation of state in Heisenberg ferromagnets).

Correlations in Fourier space

- We consider instead the Fourier transform of $C_4(\mathbf{r}|q)$

$$\hat{C}_4(\mathbf{k}|q^2 < q_{EA}^2) \propto k^{\theta(q)-D} + \dots \quad \hat{C}_4(\mathbf{k}|q^2 > q_{EA}^2) \propto \frac{1}{k^2 + \xi_q^{-2}}$$

- We use the shorthand

$$F_q = \hat{C}_4(\mathbf{k}_{\min}|q) \quad F_q^{(n)} = \hat{C}_4(n\mathbf{k}_{\min}|q)$$

- Droplet and RSB disagree in the precise form of $\theta(q)$
- Yet, both theories agree that a crossover appears in F_q for finite L

$$F_q \sim L^{D-\theta(q)} \quad \text{for } |q| < q_{EA} \quad \longrightarrow \quad F_q \sim 1 \quad \text{for } |q| > q_{EA}$$

- For large L the crossover becomes a phase transition where

$$\xi_q^{L=\infty} \propto (q^2 - q_{EA}^2)^{-\hat{\nu}}$$

(analogous to the study of the equation of state in Heisenberg ferromagnets).

- From very general RG arguments we can derive a scaling law:

$$\theta(q_{EA}) = 2/\hat{\nu}.$$

The computation of q_{EA} (I)

- According to Finite-Size Scaling,

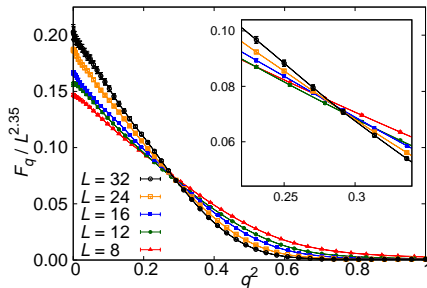
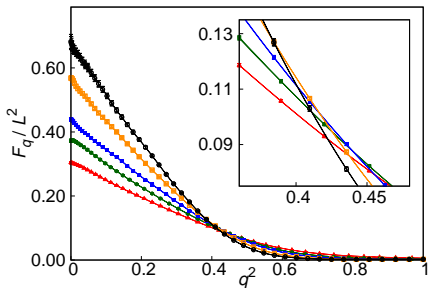
$$F_q^{(n)} \simeq L^{D-\theta(q_{EA})} G_n(L^{1/\hat{\nu}}(q - q_{EA}))$$

The computation of q_{EA} (I)

- According to Finite-Size Scaling,

$$F_q^{(n)} \simeq L^{D-\theta(q_{EA})} G_n(L^{1/\hat{\nu}}(q - q_{EA}))$$

- We consider F_q/L^y , with $y < D - \theta(0)$.
- In the large- L limit, these quantities diverge for $|q| < q_{EA}$ but vanish for $|q| > q_{EA}$.



The computation of q_{EA} (II)

- We consider pairs $(L, 2L)$.
- The crossing points $q_{L,y}$ scale as

$$q_{L,y} = q_{EA} + A_y L^{1/\hat{\nu}} \quad (**)$$

The computation of q_{EA} (II)

- We consider pairs $(L, 2L)$.
- The crossing points $q_{L,y}$ scale as

$$q_{L,y} = q_{EA} + A_y L^{1/\hat{\nu}} \quad (**)$$

- We can use this formula to compute the value of q_{EA} .

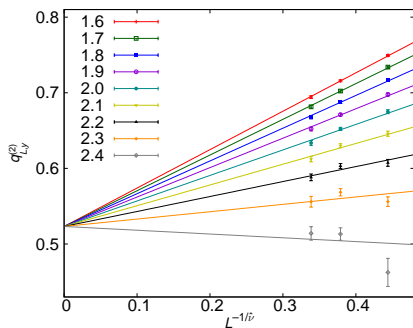
The computation of q_{EA} (II)

- We consider pairs $(L, 2L)$.
- The crossing points $q_{L,y}$ scale as

$$q_{L,y} = q_{EA} + A_y L^{1/\hat{\nu}} \quad (**)$$

- We can use this formula to compute the value of q_{EA} .
- For a given y , we have only three crossings: $(8,16)$, $(12,24)$ $(16,32)$.

The computation of q_{EA} (II)

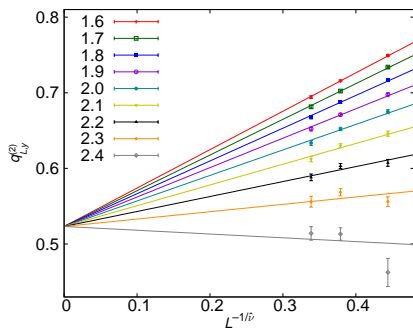


- We consider pairs $(L, 2L)$.
- The crossing points $q_{L,y}$ scale as

$$q_{L,y} = q_{EA} + A_y L^{1/\hat{\nu}} \quad (**)$$

- We can use this formula to compute the value of q_{EA} .
- For a given y , we have only three crossings: $(8,16)$, $(12,24)$, $(16,32)$.
- We perform a joint fit to $(**)$ for several values of y .

The computation of q_{EA} (II)

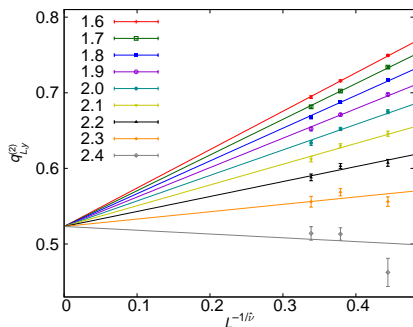


- We consider pairs $(L, 2L)$.
- The crossing points $q_{L,y}$ scale as

$$q_{L,y} = q_{EA} + A_y L^{1/\hat{\nu}} \quad (**)$$

- We can use this formula to compute the value of q_{EA} .
- For a given y , we have only three crossings: $(8,16)$, $(12,24)$, $(16,32)$.
- We perform a joint fit to $(**)$ for several values of y .
- Obviously, the intersections for different y are correlated, but we can control this by computing their covariance matrix.

The computation of q_{EA} (II)



$$q_{EA} = 0.52(3), \quad 1/\hat{\nu} = 0.39(5)$$

- We consider pairs $(L, 2L)$.
- The crossing points $q_{L,y}$ scale as

$$q_{L,y} = q_{EA} + A_y L^{1/\hat{\nu}} \quad (**)$$

- We can use this formula to compute the value of q_{EA} .
- For a given y , we have only three crossings: $(8,16)$, $(12,24)$, $(16,32)$.
- We perform a joint fit to $(**)$ for several values of y .
- Obviously, the intersections for different y are correlated, but we can control this by computing their covariance matrix.

Conclusions

- We have shown how to assess thermalisation in parallel-tempering simulations and efficiently allocate CPU time.

Conclusions

- We have shown how to assess thermalisation in parallel-tempering simulations and efficiently allocate CPU time.
- We have studied the connected spatial correlation functions in the low-temperature phase of the 3D Edwards-Anderson-Ising spin glass.

Conclusions

- We have shown how to assess thermalisation in parallel-tempering simulations and efficiently allocate CPU time.
- We have studied the connected spatial correlation functions in the low-temperature phase of the 3D Edwards-Anderson-Ising spin glass.
- We use FSS arguments to provide the first reliable determination of q_{EA} and of the exponent $1/\hat{\nu}$ that rules finite-size effects.

Conclusions

- We have shown how to assess thermalisation in parallel-tempering simulations and efficiently allocate CPU time.
- We have studied the connected spatial correlation functions in the low-temperature phase of the 3D Edwards-Anderson-Ising spin glass.
- We use FSS arguments to provide the first reliable determination of q_{EA} and of the exponent $1/\hat{\nu}$ that rules finite-size effects.
- Other physical results:
 - We have established a time-length dictionary, relating non-equilibrium and equilibrium.
 - We conclude that RSB is the appropriate theoretical framework for experimentally relevant length scales.